

Solar charge controller for battery using buck-boost converter

Nguyen Van Huynh

Thai Nguyen University of Technology, Thai Nguyen, Viet Nam

Date of Submission: 05-05-2024

Date of Acceptance: 15-05-2024

ABSTRACT: Charger controllers for solar batteries are becoming more and more popular these days. However, these control structures are generally divided into two categories: maximum power point tracking (MPPT) control and charge control. This leads to considerable losses in small capacity equipment. On the other hand, when using a converter, it will be challenging to implement MPPT algorithms. This paper presents a control solution using a buck-boost converter that can satisfy multiple voltage ranges of batteries and solar cells while still optimizing the working capacity of the system.

KEYWORDS: MPPT, P&O Algorithm, Buck - Boost Converter & DC - DC Converter.

I. INTRODUCTION

Solar panels, including many solar cells, are semiconductor elements containing on the surface a large number of light sensors, photodiodes, converting light radiation into electrical energy. This conversion is done according to the photoelectric effect. Solar cells operate according to the I-V and P-V nonlinear properties, which vary linearly with solar radiation and operating temperature of photovoltaic (PV) cells [1-5].

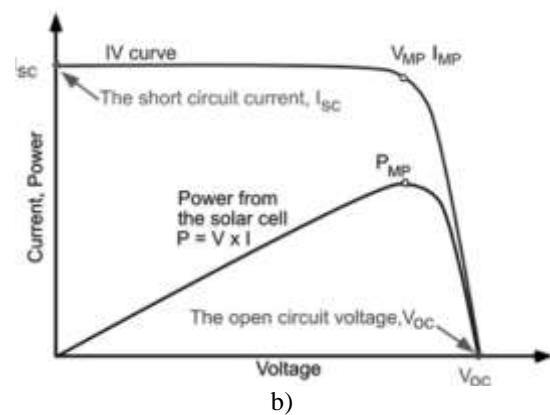
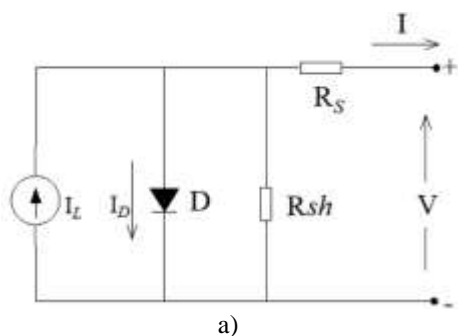


Figure 1: a) Equivalent circuit of Photovoltaic Cells.

b) IV and PV Working Characteristics of Solar Cells.

Figure 1a. depicts an equivalence circuit of a photovoltaic cell. The voltage-current equation of a photovoltaic cell in a solar cell is given as below:

$$I_{PV} = I_{PH} - I_S \left[\exp \left(\frac{q(V_{PV} + I_{PV}R_S)}{kT_c A} \right) - 1 \right] - \frac{V_{PV} + I_L R_S}{R_{SH}} \quad (1)$$

The I_{PH} photovoltaic current of a PV cell depends on the solar radiation and the working temperature of the PV cell, which is determined as follows:

$$I_{PH} = I_{SC}^{STC} + K_i (T_{PV} + T_{PV}^{STC}) \frac{\lambda}{\lambda^{STC}} \quad (2)$$

The saturation current of the PV cell, I_S varies with the temperature of the PV cell, which is determined by the following formula:

$$I_S = I_{RS} \left(\frac{T_C}{T_{PV}^{STC}} \right)^3 \left[\exp \frac{qE_\lambda \left(\frac{1}{T_{PV}^{STC}} - \frac{1}{T_C} \right)}{kA} \right] \quad (3)$$

The MPPT algorithm [6-10] has obtained very satisfactory results and has been widely applied. One of the algorithms that has a remarkable feature

is the P&O algorithm. The power electronic converters make the adjustment of the system working point more flexible. With chargers, the output voltage of the converter is assumed to be fixed and equal to the battery voltage, so the problem becomes complicated. Most converters mentioned in the literature [12-14] only focus on solving the MPPT problem without mentioning valve switching.

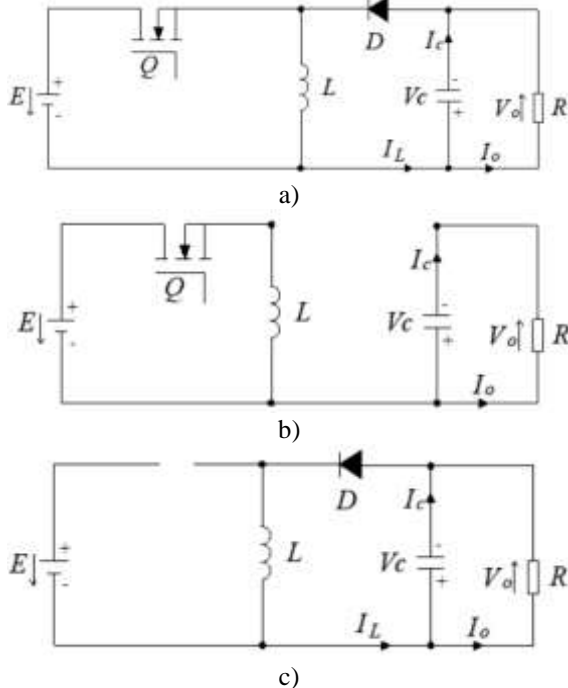


Figure 2: a) Principle Diagram of Buck – Boost Converter, b) Q on and D off, c) Q off and D on

A DC-DC buck-boost converter is shown in Figure 2a. The buck-boost converter works with two states of the valve Q. In the first half-cycle, when Q is closed, the source energy E is accumulated for inductor L, as shown in Figure 2b. In the second half-cycle, when Q is open, inductance L discharges and accumulates energy through diode D into the load, as shown in Figure 2c. The buck-boost converter that is being studied only considers the converter's operation in the continuous mode (CCM). When the valve is closed, the current in the circuit follows the following equation:

$$L \frac{di_L}{dt} = V_{in}(t) \quad (4)$$

The amount of the current increase is determined as below:

$$\Delta i_{L,on} = \int_0^{T_{on}} di_L \quad (5)$$

From (4) and (5) we have:

$$\Delta i_{L,on} = \int_0^{T_{on}} \frac{V_{in}(t)}{L} dt \quad (6)$$

Operation of the converter when the valve is closed is given by

$$L \frac{di_L}{dt} = V_{out} \quad (7)$$

The amount of the current drop during this period is calculated as

$$\Delta i_{L,off} = \int_0^{T_{off}} di_L \quad (8)$$

From (7) and (8) we have:

$$\Delta i_{L,off} = \int_0^{T_{off}} \frac{V_{out}}{L} dt = \frac{V_{out} T_{off}}{L} \quad (9)$$

The total current variation in the steady-state is zero. Therefore, $\Delta i_{L,on} = \Delta i_{L,off}$. From (6) and (9), we have:

$$\int_0^{T_{on}} \frac{V_{in}(t)}{L} dt = \frac{V_{out} T_{off}}{L} \quad (10)$$

From (10), we see that V_{out} is the voltage of the applied battery. Due to the variation of the battery voltage is slow, V_{out} = V_{BAT} = const can be considered. Accordingly, have:

$$\int_0^{T_{on}} V_{pv}(t) dt = V_{BAT} T_{off} \quad (11)$$

The relationship between VPV and IPV is shown in (1). In other words, VPV is a variable depending on the working point on the P-V curve, as shown in Figure 1b.

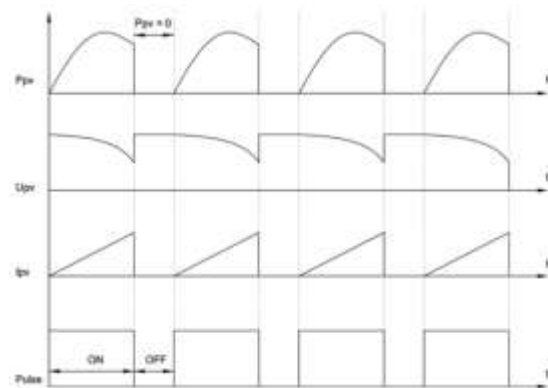


Figure 3: Operation of a Buck-Boost Converter Connected to Solar Cells.

Therefore, during one valve's opening and closing cycle, the power of the system varies continuously and does not work steadily at the maximum, as shown in Figure 3. When the valve is open, the battery's energy is accumulated into the inductor. When the valve is closed, the solar panel is disconnected from the converter. This reduces the actual working capacity of the PV panels. The average capacity of the PV panels depends on T_{on} and T_{off}. If T_{on} >> T_{off}, the operating time of the battery would take up most of the working cycle, so the maximum power is

achieved. To solve this problem, a large enough capacitor is added to store the panel's energy while the valve was in closed mode. Such a capacitor, however, would not be suitable for compact systems that require flexibility. This paper proposes a method of controlling the valve opening and closing process so that the power of the system is optimal.

II. CONTROL STRUCTURE

1. System Structure

The proposed system structure is depicted in figure 4. The solar panels are connected to a buck-boost converter with an inverting topology. The converter output is connected to a battery. DC loaders may be connected in parallel with the battery for other purposes.

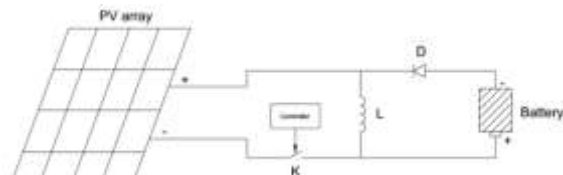


Figure 4: The Charging System Structure uses a Buck-Boost Circuit.

The control method for the K-switch is similar to the peak current control method described in the literature [15,16]. Techniques for implementing such a system are simple and implemented in many power electronic converter systems [17].

2. Peak Current Control Algorithm

DC-DC controllers can all be controlled by the peak current method [6]. The principle of this approach is that the valve switching occurs when the current on the inductor reaches a preset peak value. With this method, the control frequency will vary depending on the load and inductor of the converter. This method is quite simple and is often implemented on hardware rather than on digital

platforms. Hence, its fabrication is quite simple. The control algorithm of this method is described in figure 5. The principle of this method uses an inductor current feedback, I_L . When the current I_L is less than a preset value, I_{set} the valve will switch from closed to open state. When the voltage U_{pv} is less than a preset value, U_{set} the valve will switch from an open to a closed state.

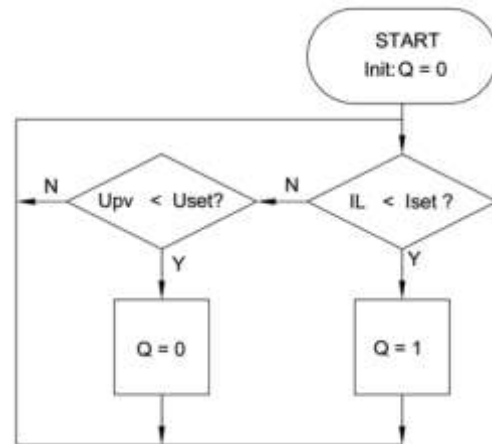


Figure 5: Peak Current Control Algorithm.

The advantage of this approach is that it does not consider the operating mode of the converter. The converter can operate in a buck or boost mode depending on battery voltage. The U_{set} and I_{set} values provided by the improved P&O algorithm will be presented in the following sections.

3. Improved P&O Algorithm

The improved P&O algorithm relies on the change of power and voltage before and after correction to predict the current operating point of the solar panel. This algorithm has many variations by adding or changing several evaluation criteria, thereby changing the amount of control error in order to quickly approach the maximum power point [18,19,20].

Table 1: Interpret the Meaning and Control Method of P&O Algorithm.

Position	Variation of Operating Power (ΔP)	Variation of Operating Voltage (ΔV)	System Working Tendency	Control Tendency
1	$\Delta P < 0$	$\Delta V < 0$	Position 1	D decreases
2	$\Delta P < 0$	$\Delta V > 0$	Position 2	D decreases
3	$\Delta P > 0$	$\Delta V < 0$	Position 3	D increases
4	$\Delta P > 0$	$\Delta V > 0$	Position 4	D increases

This algorithm can be easily implemented on practical embedded systems [11]. Table 1 describes how the basic P&O algorithm works.

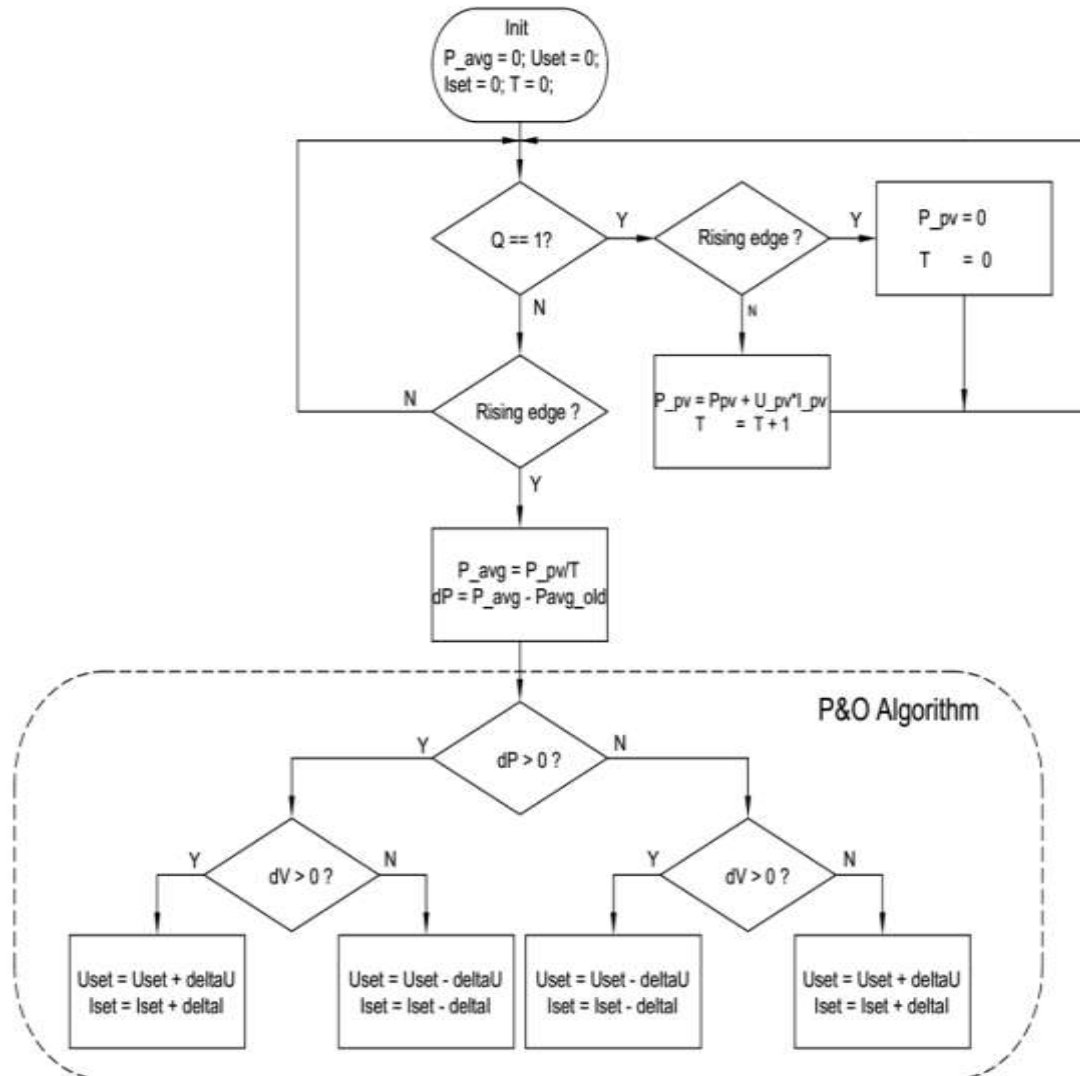


Figure 6: Customizable P&O Algorithm for Buck - Boost Converter.

With the operating principle of the basic P&O algorithm, this paper proposes a peak-current (I_{peak}) control method for a buck-boost converter, as shown in figure 6. The algorithm identifies two switching points, U_{set} and I_{set} , by calculating the average power in one open valve cycle, P_{avg} , and the average switching voltage, U_{avg} , at the beginning of each cycle, using the following formula:

$$\begin{cases} U_{avg} = U_{peak} - U_{set} \\ P_{avg} = \frac{\sum_{T=0}^n V_{pv} I_{pv}}{T} \end{cases} \quad (12)$$

The values obtained from (12) will be used to implement the P&O algorithm described in the previous section.

III. SIMULATION

1. Simulation Diagram

The simulation model was built on Matlab/Simulink software, as shown in figure 7. The simulated panels' parameters are described in table 2.

Table 2: Solar Panel Parameters

Parameter	Symbol	Value	Unit
Maximum power	Pmax	29	W
Open-circuit voltage	Uoc	7.2	V
Short-circuit current	Isc	4	A
Voltage at the maximum point	Vmp	6	V
Current at the maximum point	Imp	3	A
Number of serial panels	Ns	1	
Number of parallel panels	Np	1	

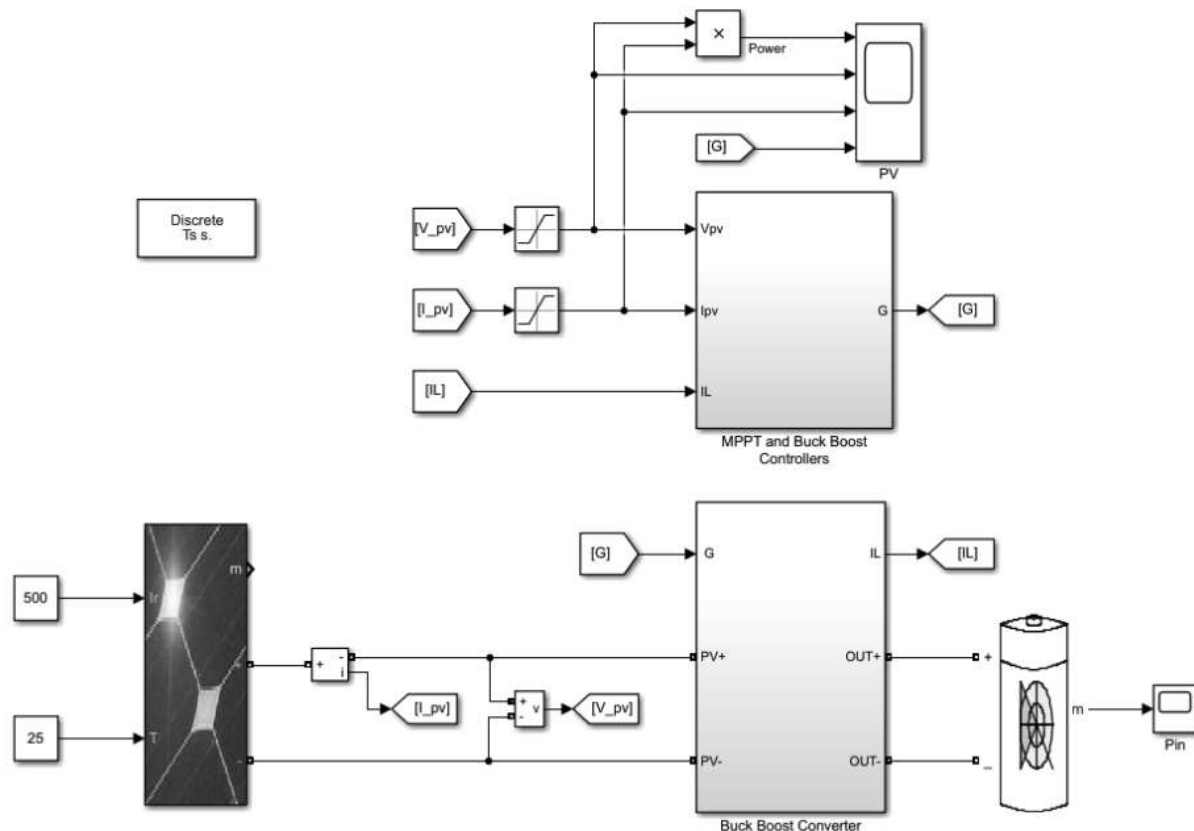


Figure 7: Simulation Diagram of the System.

2. Simulation Results

Case 1: In this simulation, the controller is evaluated with radiation intensity 500W/m^2 , $\Delta U = 0.1\text{V}$, $\Delta I = 0.1\text{A}$. The system reaches the steady-

state after 1.05s (figure 8., figure 9.), with reference voltage $U_{set} = 3\text{V}$ and reference current $I_{set} = 2.25\text{A}$.

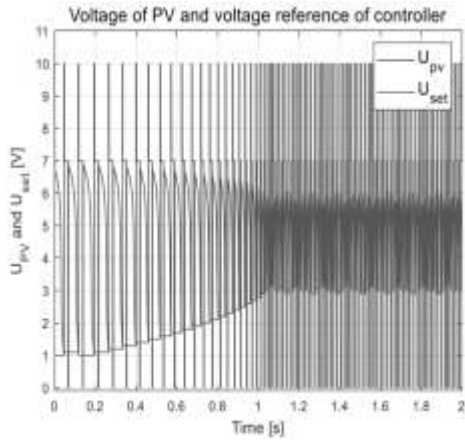


Figure 8: Voltage of the PV and Reference Voltage of the Controller.

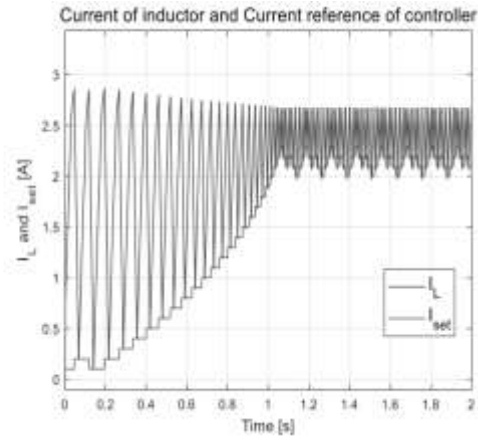


Figure 9: Current of the Inductor and the Reference Current of the Controller.

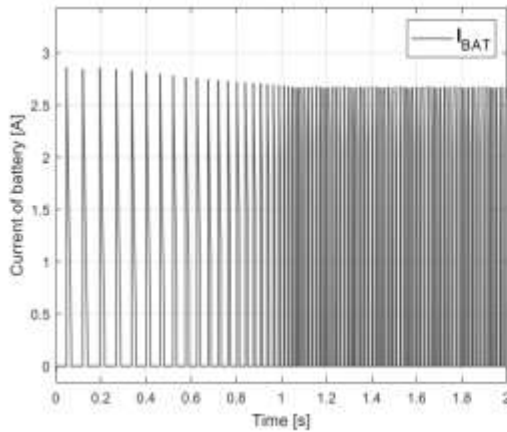


Figure 10: Current of the Battery.

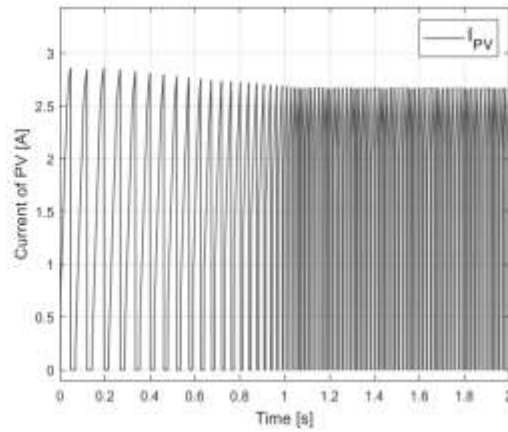


Figure 11: Current of the PV.

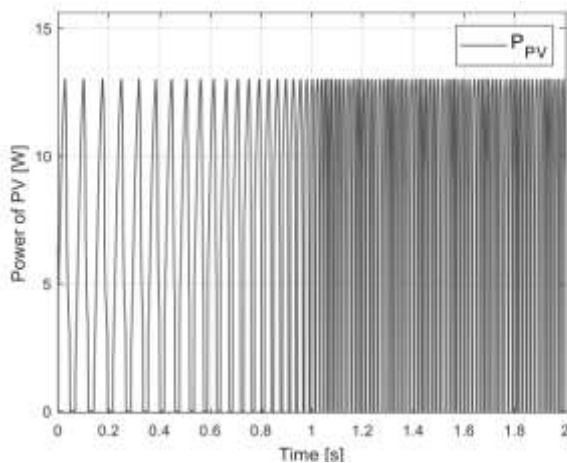


Figure 12: Power of the PV.

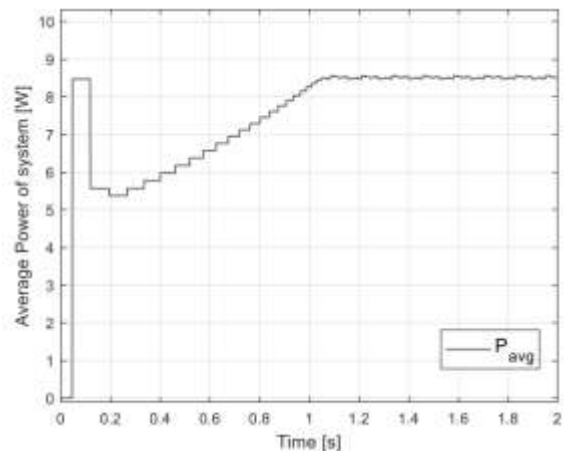


Figure 13: Average Power of Solar Panels.

The average power of the system is approximately $P_{avg} = 12W$ (Figure 13.), while the maximum power of the PVpanels $P_{max} = 14.9W$ at radiation intensity $I_r = 500W/m^2$. The system

achieves 80% efficiency.

Case 2: Power of the converter for different battery voltages. In this simulation, the operation of the system is evaluated with different battery voltage

ranges. There are three battery voltages to be used: 3.7V, 12V, and 24V. Figure 14. shows the operations of the controller for different battery voltages, where all three considered voltages

result in an average power of about 12W. However, for systems with lower battery voltages, the convergence time of the algorithm is slower due to the longer inductor charging.

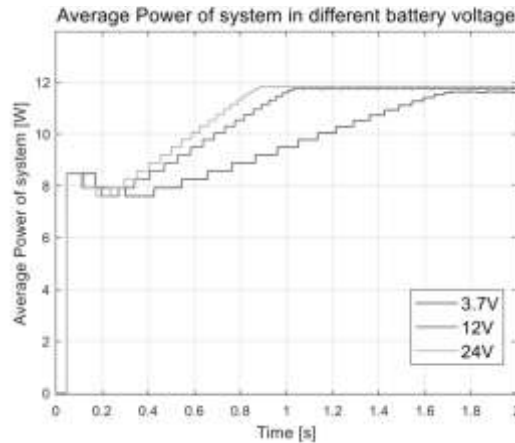


Figure 14: The Average PV Power Corresponds to Different Charging Voltages. Conversion efficiency at different battery voltages is given in Table 3.

Table 3: Conversion Efficiency at Different Battery Voltages

Battery Voltages	Average Power	Efficiency
3.7V	11.5W	77%
12V	11.8W	79%
24V	11.9W	80%

IV. CONCLUSIONS

Simulation results show that the system is satisfied with different voltage ranges of batteries and solar panels. Besides, the algorithm allows optimizing the system's power up to 80% of the maximum power of the PV panels. The implemented control scheme has improved the working capacity of the charging control system for batteries using solar panels.

ACKNOWLEDGEMENTS

This research was funded by Thai Nguyen University of Technology, No. 666, 3/2 Street, Thai Nguyen, Viet Nam.

SYMBOLS

I_{PH}	Photoelectric current
I_s	Saturated current
q	Atomic charge
k	Boltzmann's constant
T_C	Working temperature of the photovoltaic cell
A	Ideal constant of semiconductor materials

R_{SH}	Parallel resistance (shunt)
R_s	Serial resistance
I_{SC}^{STC}	Short-circuit current of the photoelectric cells at 25°C and 1kW/m ²
T_{PV}	The working temperature of the photovoltaic cells (°C)
K_i	Short-circuit current temperature coefficient of photovoltaic cells
λ^{STC}	Solar radiation 1kW/m ²
I_{RS}	Current flows through the internal parallel resistance RSH
E_λ	Distance energy of semiconductors of photovoltaic cells
T_{PV}^{STC}	Standard temperature of the photovoltaic cell °C

REFERENCES

- [1]. Petreuş, D., Fărcaş, C., & Ciocan, I. (2008). Modelling and simulation of photovoltaic cells. Acta

- TechnicaNapocensisElectronics and Telecommunications, 49(1), 42-47.
- [2]. Sheng, X., Broderick, L. Z., &Kimerling, L. C. (2014). Photonic crystal structures for light trapping in thin-film Si solar cells:Modeling, process and optimizations. *Optics Communications*, 314, 41-47.
- [3]. Bouzidi, K., Chegaar, M. A. B. A., &Bouhemadou, A. (2007). Solar cells parameters evaluation considering the series andshunt resistance. *Solar Energy Materials and Solar Cells*, 91(18), 1647-1651.
- [4]. Chegaar, M., Hamzaoui, A., Namoda, A., Petit, P., Aillerie, M., &Herguth, A. (2013). Effect of illumination intensity on solarcells parameters. *Energy Procedia*, 36, 722-729.
- [5]. Bouzidi, K., Chegaar, M., &Aillerie, M. (2012). Solar cells parameters evaluation from dark IV characteristics. *EnergyProcedia*, 18, 1601-1610.
- [6]. Hallworth, M., &Shirsavar, S. A. (2011). Microcontroller-based peak current mode control using digital slopecompensation. *IEEE Transactions on Power Electronics*, 27(7), 3340-3351.
- [7]. Liu, F., Duan, S., Liu, F., Liu, B., & Kang, Y. (2008). A variable step size INC MPPT method for PV systems. *IEEETransactions on industrial electronics*, 55(7), 2622-2628.
- [8]. De Brito, M. A. G., Galotto, L., Sampaio, L. P., e Melo, G. D. A., &Canesin, C. A. (2012). Evaluation of the main MPPTtechniques for photovoltaic applications. *IEEE transactions on industrial electronics*, 60(3), 1156-1167.
- [9]. Ahmed, J., & Salam, Z. (2015). An improved perturb and observe (P&O) maximum power point tracking (MPPT) algorithmfor higher efficiency. *Applied Energy*, 150, 97-108.
- [10]. Kollimalla, S. K., & Mishra, M. K. (2014). Variable perturbation size adaptive P&O MPPT algorithm for sudden changes inirradiance. *IEEE Transactions on Sustainable Energy*, 5(3), 718-728.
- [11]. Khaehintung, N., Wiangtong, T., &Sirisuk, P. (2006, October). FPGA implementation of MPPT using variable step-size P&Oalgorithm for PV applications. In 2006 International Symposium on Communications and Information Technologies (pp. 212-215). IEEE.
- [12]. Choudhary, D., & Saxena, A. R. (2014). Dc-Dc buck-converter for mppt of pv system. *International Journal of EmergingTechnology and Advanced Engineering*, 4(7), 813-821.
- [13]. Singh, S. N. (2017). Selection of non-isolated DC-DC converters for solar photovoltaic system. *Renewable and SustainableEnergy Reviews*, 76, 1230-1247.
- [14]. Prasad, S. Y., Chhetri, B. B., Adhikary, B., &Bista, D. (2010, September). Microcontroller based intelligent DC/DC converterto track Maximum Power Point for solar photovoltaic module. In 2010 IEEE Conference on Innovative Technologies for anEfficient and Reliable Electricity Supply (pp. 94-101). IEEE.
- [15]. Wu, K. C. (2004). A comprehensive analysis of current-mode control for DCM buck-boost converters. *IEEE Transactions onIndustrial Electronics*, 51(3), 733-735.
- [16]. Cooke, P. (2000, February). Modeling average current mode control [of power convertors]. In APEC 2000. Fifteenth AnnualIEEE Applied Power Electronics Conference and Exposition (Cat. No. 00CH37058) (Vol. 1, pp. 256-262). IEEE.
- [17]. Chattopadhyay, S., & Das, S. (2006). A digital current-mode control technique for DC-DC converters. *IEEE Transactions onPower Electronics*, 21(6), 1718-1726.
- [18]. Femia, N., Petrone, G., Spagnuolo, G., & Vitelli, M. (2004, June). Optimizing sampling rate of P&O MPPT technique. In 2004IEEE 35th Annual Power Electronics Specialists Conference (IEEE Cat. No. 04CH37551) (Vol. 3, pp. 1945-1949). IEEE.
- [19]. Femia, N., Petrone, G., Spagnuolo, G., & Vitelli, M. (2009). A technique for improving P&O MPPT performances of doublestage grid-connectedphotovoltaic systems. *IEEE transactions on industrial electronics*, 56(11), 4473-4482.
- [20]. Femia, N., Petrone, G., Spagnuolo, G., & Vitelli, M. (2004, June). Optimizing duty-cycle perturbation of P&O MPPTtechnique. In 2004 IEEE 35th Annual Power Electronics Specialists Conference (IEEE Cat. No. 04CH37551) (Vol. 3, pp.1939-1944). IEEE.